



**UNIVERSITY OF LEEDS**

This is a repository copy of *Nanosensors for the detection of hydrogen peroxide*.

White Rose Research Online URL for this paper:

<http://eprints.whiterose.ac.uk/101072/>

Version: Accepted Version

---

**Article:**

Clausmeyer, J, Actis, P [orcid.org/0000-0002-7146-1854](https://orcid.org/0000-0002-7146-1854), Córdoba, AL et al. (2 more authors) (2014) Nanosensors for the detection of hydrogen peroxide. *Electrochemistry Communications*, 40. pp. 28-30. ISSN 1388-2481

<https://doi.org/10.1016/j.elecom.2013.12.015>

---

© 2013 Elsevier B.V. Published by Elsevier B.V. All rights reserved. This manuscript version is made available under the CC-BY-NC-ND 4.0 license <http://creativecommons.org/licenses/by-nc-nd/4.0/>.

**Reuse**

This article is distributed under the terms of the Creative Commons Attribution-NonCommercial-NoDerivs (CC BY-NC-ND) licence. This licence only allows you to download this work and share it with others as long as you credit the authors, but you can't change the article in any way or use it commercially. More information and the full terms of the licence here: <https://creativecommons.org/licenses/>

**Takedown**

If you consider content in White Rose Research Online to be in breach of UK law, please notify us by emailing [eprints@whiterose.ac.uk](mailto:eprints@whiterose.ac.uk) including the URL of the record and the reason for the withdrawal request.



[eprints@whiterose.ac.uk](mailto:eprints@whiterose.ac.uk)  
<https://eprints.whiterose.ac.uk/>

# Nanosensors for the Detection of Hydrogen Peroxide

Jan Clausmeyer<sup>a</sup>, Paolo Actis<sup>b</sup>, Ainara López Córdoba<sup>b</sup>, Yuri Korchev<sup>b</sup>,  
Wolfgang Schuhmann<sup>a\*</sup>

<sup>a</sup> Analytische Chemie - Elektroanalytik & Sensorik, Ruhr-Universität Bochum  
Universitätsstr. 150, D-44780 Bochum, Germany  
Phone: +49 234 32 26200; Fax: +49 234 32 14683, E-Mail: wolfgang.schuhmann@rub.de

<sup>b</sup> Division of Medicine, Imperial College London, London W12 0NN, United Kingdom

## Abstract

Prussian Blue (PB) deposited on a nanoelectrode is the basis for an amperometric hydrogen peroxide sensor. Carbon nanoelectrodes, fabricated from pyrolytic decomposition of butane within a quartz nanopipette, were electrochemically etched and PB was deposited in the formed nanocavity. This procedure significantly increased the stability of PB films while maintaining a high mean sensitivity of  $50 \text{ A}\cdot\text{mol}^{-1}\cdot\text{l}\cdot\text{cm}^{-2}$  for  $\text{H}_2\text{O}_2$  detection at  $-50 \text{ mV}$  vs.  $\text{Ag}/\text{AgCl}$  ( $0.1 \text{ M Cl}^-$ ) at neutral pH value. Hydrogen peroxide was selectively quantified in the concentration range from  $10 \mu\text{M}$  to  $3 \text{ mM}$ . We envision the application of these nanosensors to the intracellular monitoring of oxidative stress in living cells.

## Introduction

Detection of analytes in confined environments, such as microdroplets or living cells, requires the development of robust nanodevices amenable to selective and analytical detection of biologically relevant molecules. Owing to their high sensitivity [1], low response time and the possibility for high-resolution mapping of analyte distributions, amperometric sensors based on micro- or nanoelectrodes allow for the real-time investigation of biological processes at the single-cell level [2,3]. The determination of reactive oxygen and nitrogen species [4–7] (ROS, RNS) from single cells has gained increasing attention. ROS and RNS are released from cells at high metabolism conditions and they are believed to play a key role in a number of pathogenic conditions including cancer development, neurodegeneration and heart failure [8,9]. To identify the contribution of specific compounds to overall oxidative stress, new selective and nano-sized sensors have to be developed. Here, we report the modification of nanoelectrodes with Prussian Blue (PB), a well-known selective electrocatalyst for the reduction and oxidation of  $\text{H}_2\text{O}_2$  [10,11], which is one of the most important ROS [12]. However, the stability of PB films, especially in neutral and alkaline media, has remained

critical. Common strategies to improve the longevity of the sensor devices on macroscopic electrodes are heat treatment [13], entrapment of PB in carbon inks/pastes [14] and coating with polymer films [15]. Microsensors for H<sub>2</sub>O<sub>2</sub> were based on electrodes fabricated from carbon microfibers or metal wires [16–19]. This approach requires rather tedious manual manipulation techniques and is limited with respect to further miniaturization of the sensor. These sensors have been applied for monitoring H<sub>2</sub>O<sub>2</sub> release from cells but they cannot be utilized for intracellular detection because of the large size of the probe. We presume that existing limitations of PB-based H<sub>2</sub>O<sub>2</sub> microsensors are due to the weak adhesion of the PB film if its thickness is of similar dimensions as the diameter of the electrode. Most previous strategies for stability improvement require additional coating steps whereas the coating material itself is subject to the same limitations. In this communication, we address the stability issue of PB films on electrode surfaces and obtain a substantial additional miniaturization of H<sub>2</sub>O<sub>2</sub> sensors by electrodeposition of PB into etched nanocavities [20,21] inside of carbon nanoelectrodes fabricated by pyrolytic decomposition of a hydrocarbon gas within a quartz nanopipette [22–24].

## Materials and Methods

Preparation of carbon nanoelectrodes was described in detail elsewhere [22]. In short, quartz capillaries (inner diameter 0.9 mm, outer diameter 1.2 mm) (Sutter Instruments) were pulled to fine tips with a P-2000 laser puller (Sutter Instruments). Parameters typically used were Heat 900, Filament 3, Velocity 45, Delay 130 and Pull 90. The obtained nanopipettes were connected to a butane/propane (80:20) container (Campingaz) and inserted into a second, quartz tube which was connected to an Ar cylinder. Under inert atmosphere, the capillaries were heated with a jet torch for typically 20 s. All electrochemical measurements were carried out at room temperature using a two-electrode configuration with a chloridized silver wire as the counter-reference electrode. Solutions were prepared with ultrapure water (SG). Cyclic voltammograms (CV) were recorded with a VA-10 potentiostat (npi) whereas for calibration curves a L/M-EPC 7B Whole Cell/ Patch Clamp amplifier (List-Medical) was employed. The current signals were filtered with an in-built analog 100 Hz and 1 kHz lowpass filters, respectively, and additionally with a digital 50 Hz lowpass filter. In all CVs the scan rate was 200 mV/s. All reported potentials refer to the Ag/AgCl pseudo-reference electrode in the corresponding solution containing Cl<sup>-</sup> (either 0.01 M, 0.1 M or 0.2 M, depending on the experiment). The initial electrode radius  $r$  was estimated from the steady-state current  $i_{ss}$  at -0.5 V in 5 mM [Ru(NH<sub>3</sub>)<sub>3</sub>]Cl<sub>3</sub>, 0.1 M KCl according to the relation  $i_{ss} = 4.64 \cdot r \cdot F \cdot c \cdot D$  with  $F$  the Faraday constant,  $c$  the concentration and  $D$  the diffusion coefficient [25]. All electrodes exhibited a radius between 88 nm and 153 nm. Electrochemical etching was performed by means of CV from 0 V to 2 V in 0.1 M KOH, 10 mM KCl for typically 15 cycles until the

formation of a cavity occurred. Electrochemical deposition of PB was achieved by potential cycling from 0.6 V to 0.4 V for 10 cycles in 0.1 mM FeCl<sub>3</sub> and 1 mM K<sub>3</sub>[Fe(CN)<sub>6</sub>] in 0.1 M HCl, 0.1 M KCl. After deposition the PB film was activated by cycling in the same potential range in only 0.1 M HCl, 0.1 M KCl for at least 100 cycles. Standard external K<sup>+</sup> solution contained 150 mM NaCl, 6 mM KCl, 1 mM MgCl<sub>2</sub>, 1.5 mM CaCl<sub>2</sub>, 5 mM glucose and 10 mM HEPES pH 7.2. For the calibration curves, the concentration of H<sub>2</sub>O<sub>2</sub> stock solution was verified by titration with KMnO<sub>4</sub>. SEM imaging of nanoelectrodes was conducted using an EM Quanta 3 D FEG electron microscope (FEI). SEM images showed that the RG value (e.g. the ratio between the diameter of the glass sheath and the diameter of the active electrodes) of the used carbon nanoelectrodes was smaller than 1.5.

## Results

We used carbon nanoelectrodes fabricated by laser-pulling of quartz capillaries and subsequent pyrolysis of butane/propane inside the capillary. This fast and simple process ( $\approx$  1 min per electrode) yields electrodes with tunable size from nanometers to micrometers. The electrodes have extremely pointy tips, which allows for electrochemical measurements in small volumes and high-resolution SECM imaging [23]. However, functionalization of these nanoprobe to comprise a selective electrochemical sensor renders challenging due to their small size. We have observed that the mechanical and chemical stability of films deposited on these carbon nanoelectrodes deviates drastically from the one observed on macroscopic electrodes. We overcome this limitation by electrochemically etching a nanocavity into the carbon nanoelectrodes and by electrodepositing a PB film within the nanocavity. In alkaline solution, the electrode material is etched anodically by cycling the potential to 2 V. The electrochemical properties of the resulting electrodes differ significantly from planar, disk-shaped electrodes (Figure 1). Whereas a cyclic voltammogram in a solution of [Ru(NH<sub>3</sub>)<sub>6</sub>]Cl<sub>3</sub> at an electrode before etching exhibits normal steady-state behavior due to diffusion limitation, CVs for the etched electrodes show nearly symmetrical oxidation and reduction peaks with a small peak separation (36 mV). This observation indicates the formation of a nanocavity within the carbon nanoelectrode which is surrounded by quartz glass. Upon sweeping the potential, the complete amount of soluble redox mediator inside the cavity is oxidized/reduced leading to a depletion of the current after full conversion and thus, the peak shape of the curve. The formation of a cavity is confirmed from scanning electron microscopy (SEM) images of electrodes before and after etching. After etching the contrast between the cylindrical hole and the glass sheath seems higher than the contrast between the carbon disk and the glass, suggesting the successful removal of carbon material.

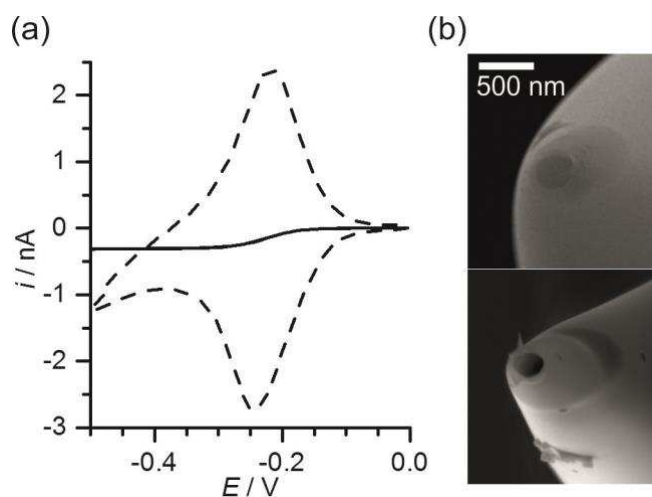


**Figure 1. Etching of carbon nanoelectrodes. CVs (a) in 5 mM  $[\text{Ru}(\text{NH}_3)_6]\text{Cl}_3$ , 0.1 M KCl at pristine electrode (solid line) and after electrochemical etching (dashed line). SEM images (b) of pristine (top) and etched electrode (bottom).**

PB was deposited electrochemically by cycling of the potential in acidic solution containing  $\text{Fe}^{3+}$  and  $[\text{Fe}(\text{CN})_6]^{3-}$ . After deposition the PB film was reduced and oxidized during more than 100 cycles in a CV to increase the stability and improve the efficiency of electron transfer (Figure 2). This “activation” process is interpreted as the incorporation of  $\text{K}^+$  ions into the crystal lattice of PB which converts the material into its more stable form [11]. An attempt to perform the activation on an electrode where the PB was deposited on the planar nanoelectrode prior to etching is shown in the inset of Figure 2. The current peaks attributed to the reduction of PB to Prussian White and subsequent re-oxidation deplete rapidly with increasing number of cycles. This result reflects the poor stability and low adhesion of the deposited material on the flat electrode. In contrast, if the PB is buried inside a cavity (Figure 2, main graph), the voltammogram displays higher peak currents irrespective of the duration of cycling, representing the larger amount of PB and its superior stability. Additionally, peak sharpening is observed which is in agreement with the anticipated rearrangement of the PB crystal lattice indicating an increase of the electron transfer rate.

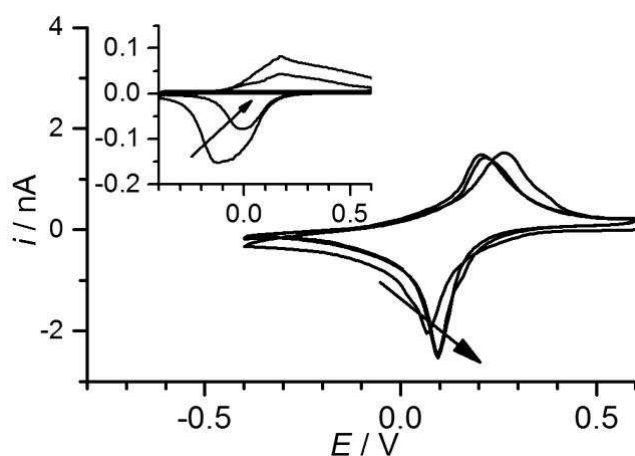


**Figure 2. Stability of PB films.** CVs in 0.1 M HCl, 0.1 M KCl after PB deposition in an etched nanocavity ( $r = 152$  nm). Inset: CV conducted after deposition of PB on a pristine electrode prior to etching ( $r = 144$  nm). CVs show the 1<sup>st</sup>, 50<sup>th</sup> and 140<sup>th</sup> cycle.

The resulting PB modified electrode constitutes a selective and sensitive sensor for the detection of  $\text{H}_2\text{O}_2$  at a potential as low as  $-50$  mV and pH 7.0. The calibration of the sensor reveals a linear response of the cathodic current with respect to  $\text{H}_2\text{O}_2$  concentration over a range of nearly three orders of magnitude, namely from  $10 \mu\text{M}$  to  $3$  mM ( $R^2$  better than 0.995). The average sensitivity of the sensors was  $50 \pm 30 \text{ A}\cdot\text{mol}^{-1}\cdot\text{l}\cdot\text{cm}^{-2}$ . The limit of detection (LOD), defined as the concentration where the signal exceeded the root-mean-square (RMS) noise by a factor of 3 was  $10 \mu\text{M}$ . The upper detection limit was determined by the stability of the PB film. At concentrations significantly exceeding  $3$  mM  $\text{H}_2\text{O}_2$  the current response of the sensor quickly decayed. However, at intermediate  $\text{H}_2\text{O}_2$  concentrations the sensors were sufficiently stable. After two hours of operation in  $0.2$  mM  $\text{H}_2\text{O}_2$  with constant turnover at  $-50$  mV the cathodic current did not decrease. With a view to ROS detection in cultured cells, the sensor was also tested in standard external  $\text{K}^+$  solution and similar sensitivity was measured. Repeated calibrations could be recorded without loss of sensitivity.

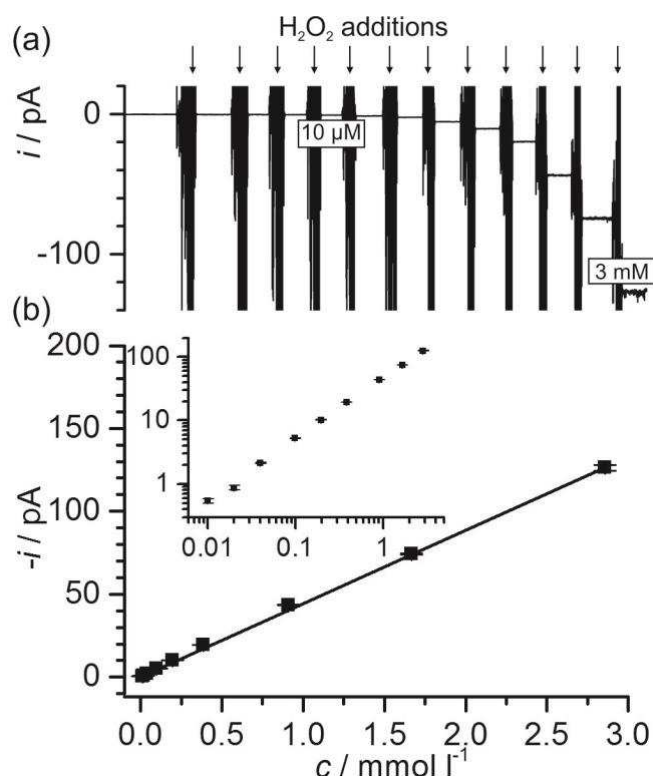


**Figure 3. Calibration of the PB  $\text{H}_2\text{O}_2$  sensor.** Detection at  $-50$  mV vs. Ag/AgCl in 50 mM phosphate buffer pH 7.0, 0.1 M KCl. Raw chronoamperometry data (a) (full x-scale 35 min). Current-concentration plot (b). Inset: Double logarithmic representation.

## Discussion

We believe that attempts for electrochemical deposition of material on small electrode surfaces is likely to result in a “basketball on a matchstick” situation where an excess of

deposited material is situated on the electrode tip [26]. As a result, the layer of deposited material is prone to dissolution and mechanical detachment from the tip. Up to now, functionalization of nanoelectrodes was mostly reported with Pt black as deposit [4,7,27]. We address the stability problem by depositing the electrocatalyst PB into an etched cavity at the apex of the nanoelectrode. The increase of chemical/electrochemical stability is likely due to the cavity preventing PB that has been dissolved or detached from being removed from the active electrode too quickly and allowing for immediate re-deposition. However, the etching creates a channel inside the glass sheath that has to be transversed by the analyte before reaching the PB film inside the cavity, resulting in a loss of sensitivity and increase of the response time due to slow planar diffusion inside the cavity. Yet, for relatively long time scales ( $t \geq l^2/4D \approx 100 \mu\text{s}$  e.g. for a cavity of depth  $l = 1 \mu\text{m}$ ) the electrode shows fast mass transport typical of hemispherical diffusion. As predicted for recessed electrodes [21] the steady-state currents observed for  $\text{H}_2\text{O}_2$  reduction are only slightly diminished with respect to the maximum theoretical value expected for ideal coplanar disk-shaped geometry. Taking the average sensitivity measured here and a typical electrode radius of 150 nm, the resulting calculated current is only three times smaller than the ideal value obtained from the equation  $i_{\text{ss}} = 4.64 \cdot r \cdot F \cdot c \cdot D$  (with  $D = 1.7 \cdot 10^{-5} \text{ cm}^2 \cdot \text{s}^{-1}$ ) [28].

## Conclusion

We present a selective amperometric nanosensor for the detection of  $\text{H}_2\text{O}_2$  based on PB deposited inside the cavity of an etched carbon nanoelectrode. Sheltering the PB in the nanocavity greatly increased the stability of the electrocatalyst while maintaining high mass transport rates. Thus, the concept may be transferred to other types of electrode modification in order to create a multitude of functional electrochemical nanosensors. In future, the  $\text{H}_2\text{O}_2$  sensor may be applied for the study of the production of ROS inside single living cells.

## Acknowledgements

This work was funded by the Engineering and Physical Sciences Research Council.

## References

- [1] J. J. Watkins, J. Chen, H. S. White, H. D. Abruña, E. Maisonhaute, C. Amatore, *Anal. Chem.* 75 (2003) 3962.
- [2] A. Schulte, W. Schuhmann, *Angew. Chem. Int. Ed.* 46 (2007) 8760.
- [3] M. Nebel, S. Grützke, N. Diab, A. Schulte, W. Schuhmann, *Angew. Chem. Int. Ed.* 52 (2013) 6335.
- [4] C. Amatore, S. Arbault, A. C. W. Koh, *Anal. Chem.* 82 (2010) 1411.
- [5] C. Amatore, S. Arbault, M. Guille, F. Lemaitre, *Chem. Rev.* 108 (2008) 2585.
- [6] S. Isik, W. Schuhmann, *Angew. Chem. Int. Ed.* 45 (2006) 7451.
- [7] Y. Wang, J.-M. Noel, J. Velmurugan, W. Nogala, M. V. Mirkin, C. Lu, M. Guille Collignon, F. Lemaitre, C. Amatore, *Proc. Natl. Acad. Sci. USA* 109 (2012) 11534.
- [8] G. Waris, H. Ahsan, *J. Carcinog.* 5 (2006) 14.
- [9] D. A. Patten, M. Germain, M. A. Kelly, R. S. Slack, *J. Alzheimers Dis.* 20 (2010) S357-S367.
- [10] W. Chen, S. Cai, Q.-Q. Ren, W. Wen, Y.-D. Zhao, *Analyst* 137 (2011) 49.
- [11] F. Ricci, G. Palleschi, *Biosens. Bioelectron.* 21 (2005) 389.
- [12] X. T. Zheng, W. Hu, H. Wang, H. Yang, W. Zhou, C. M. Li, *Biosens. Bioelectron.* 26 (2011) 4484.
- [13] A. A. Karyakin, E. A. Puganova, I. A. Budashov, I. N. Kurochkin, E. E. Karyakina, V. A. Levchenko, V. N. Matveyenko, S. D. Varfolomeyev, *Anal. Chem.* 76 (2004) 474.
- [14] F. Ricci, A. Amine, G. Palleschi, D. Moscone, *Biosens. Bioelectron.* 18 (2003) 165.
- [15] A. A. Karyakin, E. E. Karyakina, L. Gorton, *Anal. Chem.* 72 (2000) 1720.
- [16] S. Dong, G. Che, *J. Electroanal. Chem.* 315 (1991) 191.
- [17] P. Salazar, M. Martín, R. Roche, R. O'Neill, J. González-Mora, *Electrochim. Acta* 55 (2010) 6476.
- [18] M. G. Garguilo, A. C. Michael, *J. Am. Chem. Soc.* 115 (1993) 12218.
- [19] J. Li, J. Yu, *Bioelectrochemistry* 72 (2008) 102.
- [20] B. Zhang, J. Galusha, P. G. Shiozawa, G. Wang, A. J. Bergren, R. M. Jones, R. J. White, E. N. Ervin, C. C. Cauley, H. S. White, *Anal. Chem.* 79 (2007) 4778.
- [21] P. Sun, M. V. Mirkin, *Anal. Chem.* 79 (2007) 5809.
- [22] Y. Takahashi, A. I. Shevchuk, P. Novak, Y. Zhang, N. Ebejer, J. V. Macpherson, P. R. Unwin, A. J. Pollard, D. Roy, C. A. Clifford, H. Shiku, T. Matsue, D. Klenerman, Y. E. Korchev, *Angew. Chem. Int. Ed.* 50 (2011) 9638.
- [23] Y. Takahashi, A. I. Shevchuk, P. Novak, B. Babakinejad, J. Macpherson, P. R. Unwin, H. Shiku, J. Gorelik, D. Klenerman, Y. E. Korchev, T. Matsue, *Proc. Natl. Acad. Sci. USA* 109 (2012) 11540.
- [24] K. McKelvey, B. P. Nadappuram, P. Actis, Y. Takahashi, Y. E. Korchev, T. Matsue, C. Robinson, P. R. Unwin, *Anal. Chem.* 85 (2013) 7519.
- [25] C. Lefrou, R. Cornut, *ChemPhysChem* 11 (2010) 547.
- [26] L. Soleymani, Z. Fang, E. H. Sargent, S. O. Kelley, *Nature Nanotech.* 4 (2009) 844.
- [27] K. Hu, Y. Gao, Y. Wang, Y. Yu, X. Zhao, S. A. Rotenberg, E. Gökmeşe, M. V. Mirkin, G. Friedman, Y. Gogotsi, *J. Solid State Electrochem.* 17 (2013) 2971.
- [28] D. M. H. Kern, *J. Am. Chem. Soc.* 76 (1954) 4208.